



OPEN

Tyrosine phosphatase SHP2 accelerated ovarian cancer via modulating integrin/E-Cadherin/ZEB1 induced EMT

Xiaofei Li, Haibo Zhang, Jianan Dong & Juan Wang✉

This article focusing on examining the function and further, molecular function of SHP2 in ovarian cancer (OC). For the molecular mechanism, bioinformatics was applied to study the specifically expressed genes in ovarian cancer; the western blotting was applied to identify the EGF, p-SHP2, ZEB1, and E-Cadherin expressions in ovarian cancer tissue and pair adjacent tissue; then SKOV3 cells were treated with EGF and infected with E-Cadherin overexpression lentivirus, and then cells were treated with benzyl butyl phthalate and IRS-1 respectively. Detection of expression of p-SHP2, ZEB1, E-Cadherin, α 3-integrin, p-Src, p-SMAD2, Snail, Slug and SKOV3 cells of migration and invasion abilities were detected using Western blot method and cell scratch assay and Transwell assay; Progression of ovarian cancer was detected using subcutaneous tumor transplantation assay in nude mice and HE staining method and immunocyto. The bioinformatics analysis results suggested that SHP2 is highly specifically expressed and E-Cadherin, which is low specifically expressed in ovarian cancer tissues, while EGF, p-SHP2 or ZEB1 are highly expressed and E-Cadherin is low expressed in ovarian cancer tissues; Overexpression of E-Cadherin could reduce the expressions of p-SHP2, ZEB1, α 3-integrin, p-Src, p-SMAD2, Snail and Slug might has roles in alleviating the ovarian cancer development and decreasing the levels of p-SHP2 and ZEB1 in tumor samples. And E-Cadherin overexpression reduced the migration and invasion ability of SKOV3 cells. SHP2 tyrosine phosphatase enhances the ovarian cancer cells' motility and invasiveness by upregulation of the integrin/E-Cadherin switch through ZEB1 signal.

Keywords Ovarian cancer, SHP2, Eintegrin/E-Cadherin signalling pathway, Epithelial mesenchymal transition

Ovarian cancer is among the three prevalent malignant tumors in the female genital tract, and carries the highest mortality score among gynecological diseases, with 70–80% of ovarian cancer patients dying within the first 5 years after their diagnosis. Epithelial ovarian cancer makes up 85–90% of all ovarian cancers¹. Most early patients have no obvious symptoms, and it is prone to intraperitoneal implantation and metastasis in the advanced stage. In recent years, although combined treatment with surgical treatment, chemotherapy and radiotherapy has been applied, the survival rate of patients diagnosed with epithelial ovarian cancer has not been enhanced. The precise aetiology of epithelial ovarian cancer is yet to be established, although what is well understood is that a metastatic spread of the tumour is the leading cause of death among those patients diagnosed with epithelial ovarian cancer. Though the exact process of metastasis has not been fully unraveled it is known that metastasis of tumours is one of the most comprehensive processes studied till date^{2,3}.

The phosphatase SHP2 is a pivotal player in cellular signal transduction, modulating a myriad of signaling pathways through dephosphorylation, and exerting profound influences on cellular proliferation, differentiation, migration, and other biological processes. Aberrant SHP2 activity has been implicated in numerous cancer types, and it is deemed a critical target in cancer therapy. SHP2 plays an integral role in the epithelial-mesenchymal transition (EMT) process. Particularly, SHP2 affects the development of EMT and modulates tumor aggressiveness via signal transduction pathways such as EGFR and TGF- β . It regulates associated transcription factors and signaling molecules, thereby either promoting or inhibiting EMT^{4–6}.

Department of Obstetrics and Gynecology, The Fourth Hospital of Hebei Medical University, No.12, Health Road, Shijiazhuang City 050011, Hebei Province, China. ✉email: xiaohaib00@163.com

EMT facilitates the acquisition of invasive and metastatic properties by early tumor cells through the downregulation of E-cadherin expression, suppression of the Wnt pathway, disruption of the basement membrane, and subsequent entry of tumor cells into the bloodstream. Central to this process is the inhibition of E-cadherin expression, a 120-kDa calcium-dependent cell adhesion molecule that spans the cell membrane and plays a crucial role in maintaining intercellular connections. The loss of epithelial cadherin-mediated cell adhesion is universally acknowledged as a prerequisite for tumor cell invasion and metastasis. Changes in E-cadherin expression, including gene mutations, methylation of the promoter, or transcriptional repression, coupled with the influence of various signaling pathways, constitute the secondary aspect affecting the reduction of E-cadherin expression⁷. Extensive literature has demonstrated that the level of E-cadherin is a significant determinant of the prognosis in epithelial ovarian cancer. Key regulators of E-cadherin expression include SNAI1, SNAI2, ZEB1, and ZEB2. E-cadherin is intricately involved in both the initiation and progression of tumors. Consequently, given the negative correlation between E-cadherin expression and the advancement of epithelial ovarian cancer, elucidating its functional role in tumor development is essential for understanding the underlying mechanisms of this disease^{8,9}.

Epidermal growth factor (EGF) is a protein capable of initiating diverse cellular divisions, commonly found in bodily fluids and glands, and it is integral to a wide array of cellular functions, including growth, proliferation, and differentiation. The epidermal growth factor receptor (EGFR), the first identified prototype of receptor tyrosine kinases (RTKs), specifically binds to EGF, thereby transducing signals. Overexpression and point mutations of EGFR family proteins on the cancer cell surface are associated with several cancers, including ovarian cancer, making EGFR a key player in tumor occurrence, development, and prognosis. Upon EGF binding to EGFR, a cascade of downstream signaling molecules is activated, promoting tumor cell survival, proliferation, and development while inhibiting tumor cell aggregation. Given that EGFR is a known substrate of PTP1B, SHP2 is swiftly recruited to form a complex with activated EGFR in response to EGF. Gab1, in turn, is recruited to the vicinity of the activated EGFR and phosphorylated. SHP2, a protein tyrosine phosphatase, exhibits enhanced catalytic activity when its SH2 domain binds to a specific phosphorylated motif. Gab1 serves as at least an indirect substrate of SHP2 in the EGF signaling pathway^{10,11}. Ras, a small GTPase, can activate several effectors, notably the downstream mitogen-activated protein kinase ERK1/2, which is widely recognized for its involvement in cell growth, development, and survival, and has the potential to upregulate ZEB1. ZEB1, a zinc finger E-box binding homeobox 1, is a highly active transcription factor in the EMT pathway, which is a critical process in cancer invasion¹². Therefore, in our present study, we investigated the levels of SHP2 in ovarian cancer and its effects on and molecular regulation of EMT, thereby proposing novel therapeutic strategies and approaches for the treatment of ovarian cancer.

Methods

Bioinformatics analysis

The ovarian cancer-related dataset GSE54388 was selected from the GEO database. Through standardization processing, log2 was used for conversion. These Chip data were subsequently background corrected, normalized and multi probe averaged using RMA (Robust Multi-array Average). The obtained data was then processed and batch effect corrected they using the ComBat method. Differential expression analysis was performed using the DESeq2 package. First, OVCA patients' samples and normal ovarian tissue samples were categorized. The screening criteria were: DEGs with the criteria of $|log_2 \text{ Fold Change}| > 1$ and $p\text{-value} < 0.05$ were obtained by multiple testing correction through the Benjamini-Hochberg method. The DEGs were further annotated for GO and KEGG pathway enrichment analysis by ClusterProfiler. GO mainly consists of Cellular Component (CC), Molecular Function (MF) and Biological Process (BP); KEGG pathway focuses on depicting significant biological pathways. Correlation analysis was performed on differentially expressed genes to discover gene relationships.

Clinical specimens

30 cases of epithelial ovarian cancer and adjacent tissues collected in the Fourth Affiliated Hospital of Hebei Medical University, Shijiazhuang, China, from May 2022 to December 2022 were selected for clinical specimens. Among the epithelial ovarian cancers, 16 were below 50 years of age and 14 were equal to and above 50 years of age. FIGO stage: in stage I-II there were 11 patients, and in stage III-IV, 19 patients; histological differentiation: 16 cases of high and medium differentiation and 14 cases of low differentiation. Histological type: 17 serious cases of ovarian cancer, 8 mucinous cases of ovarian cancer, and 5 endometrioid cases of ovarian cancer. Chemotherapy, radiotherapy or other treatments were not provided to all the patients before surgery. All samples sought to obtain informed consent from the patients and the patients were also fully informed of the purpose, risks and benefits of the study prior to agreeing to participate in the study. The study was also approved by the Laboratory Animal Welfare Ethics Committee of the Fourth Hospital of Hebei Medical University. All methods were performed in accordance with the relevant guidelines and regulations and were in line with ARRIVE guidelines.

Cell culture

Human ovarian cancer cell line SKOV3 cells were from Wuhan Procell Life Science & Technology Co., Ltd. Normal SKOV3 cells were grown in RPMI-1640 supplemented with 10% FBS and 1% double antibody. Incubated in 37 °C with 5% CO₂. Then treated with EGF at a concentration of 20 ng/ml.

Cell treatment and grouping

The E-Cadherin virus solution used in the laboratory was purchased from Shanghai Jima Biological Co., Ltd. One day before transfection, the cells in the logarithmic growth phase were digested with trypsin, then centrifuged after digestion, the cells were then resuspended in complete 1640 medium for cell counting the density of the

cells was adjusted to 5×10^5 /ml; then added to a 12-well plate, add 1 ml of cell suspension to each well, and repeat 6 wells for each cell, and culture alternatively in a 37°C , 5% CO₂ incubator on a daily basis. After culturing for 24 h, puromycin of the next concentration was added for the next step of the experiment, and the cells should be allowed to die within 4–7 days, and it was not suitable for the time to be too long or too short; resuspend the cells and adjust to 1×10^5 /ml; then add them to the 12-well plate, add 1 ml of cell suspension to each well, and culture 6 wells for each cell in a 37°C , 5% CO₂ incubator. When the cell confluence reaches about 50%, discard the old medium in the 12-well plate, rinse twice with PBS, add the prepared virus mixture, and place it in a 37°C , 5% CO₂ incubator for routine culture; after 48 h of infection, remove the virus mixture, observe the cell status, and when the cell confluence > 80%, digest with trypsin and resuspend with RPMI-1640 medium, and replant in a 6-well plate followed by positioning it in a 37°C , 5% CO₂ incubator for regular culture. Then treated SKOV3 cells with ZEB1 agonist Benzyl butyl phthalate and SHP2 agonist IRS-1, respectively.

Cell scratch test

The cells of each group that were after 48 h culture was seeded on SKOV3 cells in a 6-well plate. Palepu and Healy recommended that the total cell fusion rate exceeded 90%, a scratch was made on the 6-well plate with a 200 μL tip of a filter tip. Subsequently, DMEM containing 10% fetal bovine serum was replaced for continued culture for 48 h. The scratch area was photographed using an electronic microscope, and images were collected at 0 and 48 h after scratching, respectively, to calculate the scratch healing percentage.

Transwell experiment

Migration assay

SKOV3 cells (5×10^4) were seeded into the upper chambers of Transwell inserts containing 200 μl of serum-free culture medium, while 600 μl of DMEM supplemented with 10% FBS was added to the lower chambers. Following a 24-h incubation, cells were washed twice with PBS. Non-migrated cells on the upper surface of the membrane were removed with a cotton swab, while migrated cells on the lower surface were fixed with 4% paraformaldehyde for 10 min, stained with 0.1% crystal violet for 6 min, and counted under an optical microscope.

Invasion assay

A mixture of 300 μl serum-free medium and 30 μl Matrigel was added to each upper chamber and incubated at 37°C for 4–5 h. Cells were digested, washed three times with serum-free medium, and counted. Matrigel-coated chambers were rinsed with serum-free medium, followed by the addition of 100 μl of cell suspension to each upper chamber and 600 μl of serum-free medium to the lower chamber. After a 20–24 h incubation at 37°C , the inserts were washed twice with PBS, fixed with 5% glutaraldehyde at 4°C , stained with 0.1% crystal violet for 30 min at room temperature. Microphotographs for the stained cells were captured using the optical microscope and the migrated and invaded cells were counted using ImageJ software.

Western blot experiment

The total protein in the tissues/cells was subjected to the extraction and lysis with RIPA lysis buffer. Protein concentration was estimated using BCA kit and enzyme marker. Finally, after the incubation of the protein lysate at 95°C for 10 min the sample was loaded and separated through SDS-PAGE and transferred to a PVDF membrane. To begin with, the blocking with 5% skimmed milk was done and then, the specific primary antibody was placed in 4°C for 12 h. The PVDF membrane transferred with protein was immersed in a square tupperware box containing the antibody and incubated for 1 h with shaking. After the incubation was completed, the secondary antibody was aspirated, TBST was added to the square tupperware box, and the membrane was placed into it so that the TBST did not go over the PVDF membrane. 5 h and the protein bands were visualized using enhanced chemiluminescence. Last of all, through Image J software the gray value of the protein was measured. The given experiment was conducted thrice and the average value was computed.

Nude mouse subcutaneous xenograft experiment

Specific-pathogen-free 12 female BALB/c nude mice with a body weight of $(18 \pm 3)\text{g}$, aged 4 weeks old were purchased from Henan Skbes Life Science and Technology Co., Ltd., housing is light 12 h, dark 12 h, temperature $(24 \pm 2)^{\circ}\text{C}$ and relative humidity of 50–60%, feeding Then free of charge, and were adaptively raised for 1 week. SKOV3 cells in the logarithmic growth phase and treated with EGF and E-Cadherin-OE were taken and their density was adjusted to $1 \times 10^4/\text{mL}$, with 6 in each group. With respect to solid tumor, 200 μl of single-cell suspension was inoculated evenly subcutaneously on the back of the neck of nude mice and sections of tumors were obtained after 20 days for further tests. Nude mice were euthanized using CO₂. Successful euthanasia was determined 20 min after the nude mice stopped breathing. The experiment was terminated when the nude mice lost their appetite during the course of the experiment. Tumor volume = Length \times (Width)² / 2.

HE staining

The transplanted tumor tissue was first fixed in 10% formalin, and then through a dehydration process, paraffin sections continue, embedding, and sectioning (thickness 3–5 μm), and routine HE staining was performed. After ethanol dehydration and xylene transparency, the slides were fixed with a coverslip, and the morphological changes of the transplanted tumor tissue were observed under an optical microscope.

Immunohistochemical staining

4 μm thick paraffin sections of tissue blocks were sectioned, and the sections were picked up with anti-Peeling Slide Glasses (MTC bio), and the slides were baked in an oven at 70°C for 30 min. After routine dewaxing to

water, the immunohistochemical detection kit was used according to the kit instructions. The citrate repair solution was used for heat repair in a pressure cooker for 3 min, and after natural cooling. Finally, the sections were washed thrice in PBS (5 min each), incubated in medical hydrogen peroxide for 10 min, and washed again thrice in PBS (5 min each); the primary antibody was applied for 1 h in a 37 °C incubator, and post washing thrice in PBS (5 min/wash), the secondary antibody was applied for 20 min in a 37 °C incubator, and the sections were; DAB was developed, and the color was controlled under a microscope, and tap water was used to stop DAB, and hematoxylin was used to restain the nucleus, and the slides were baked at 70 °C for 30 min, and the sections were dried and then fixed with neutral resin.

Statistical analysis

GraphPad Prism 9 statistical software was employed, and the data were presented as the mean \pm standard deviation. The t-test was used in the inter-group comparison while $P < 0.05$ suggested that the observed difference was statistically significant.

Results

Bioinformatics analysis results

A total of 2114 DEGs were obtained by using DESeq2 analysis and 643 were up-regulated and 840 were down-regulated. Studies showed that CDH1 was down regulated in OC tissues, while SHP2 was over expressed in OC tissues. Through expressed DEGs and biosystems, GO and KEGG analysis with ClusterProfiler showed that DEGs were significantly associated with multiple biological pathways. The online tool of GOKEGG was used in the study to show that the DEGs were closely related to Cell cycle, DNA replication, and Proteoglycans in cancer. The Information displayed in the GEO-data base set up the difference between normal vs. OC samples: the expression of SHP2 in OC samples was significantly higher than that in normal, while the CDH1 was significantly lower in OC samples. Correlation analysis revealed that SHP2 and PI3K (SMG1) were positively correlated; PI3K and ZEB1 were positively correlated; SHP2 and RAS (SYNGAP1) were positively correlated; RAS and ERK1/2 (BRD3OS) were positively correlated; ERK1/2 and ZEB1 were positively correlated; ZEB1 and E-Cadherin (CDH1) were negatively correlated; src and SMAD2 were positively correlated (Fig. 1).

The EGF/SHP2/ZEB1 signaling pathway is activated and E-Cadherin is abnormally lowly expressed in human ovarian cancer tissues

First, in the present study we analyzed the presence of EGF, p-SHP2, ZEB1 and E-Cadherin in the tissues of ovarian cancer patients and control subjects. As shown in Fig. 2, there was a statistical difference between the groups, with increased relative protein levels of EGF, p-SHP2, and ZEB1 in ovarian cancer tissues and a decreased level of E-Cadherin as compared with the level in the adjacent tissues of ovarian cancer. From this, one can deduce that in human ovarian cancer tissues the EGF/SHP2/ZEB1 signaling pathway will be expressed as well as the suppression of E-Cadherin (Fig. 2).

E-Cadherin overexpression inhibits the EGF/SHP2/ZEB1/α3-integrin signaling pathway in ovarian cancer cells thereby inhibiting the EMT process

Subsequently, we designed in vitro experiments to understand the role of E-Cadherin molecularly in ovarian cancer. Western blotting showed that the relative protein expression of p-SHP2, ZEB1, α3-integrin, p-Src, p-SMAD2, Snail and Slug was significantly higher and that of E-Cadherin was significantly lower in the EGF group compared with the control group.

The relative protein expression of E-Cadherin was significantly higher in the EGF + E-Cadherin-OE group compared with the EGF group, while the relative protein expression of p-SHP2, ZEB1, α3-integrin, p-Src, p-SMAD2, Snail and Slug was significantly lower. Compared with the EGF + E-Cadherin-OE group, the relative expressions of p-SHP2, ZEB1, α3-integrin, p-Src, p-SMAD2, Snail and Slug proteins were higher in the EGF + E-Cadherin-OE group than in the EGF + E-Cadherin-OE group, whereas the relative expressions of E Cadherin's relative expression difference was not statistically significant. The relative protein expression levels of ZEB1, α3-integrin, p-Src, p-SMAD2, Snail and Slug were significantly up-regulated in the EGF + E-Cadherin-OE + benzyl butyl phthalate group compared to the EGF + E-Cadherin-OE group, but the relative protein expression levels of p-SHP2 and E-Cadherin were significantly decreased. Relative protein expression levels did not change significantly. Relative to the EGF + E-Cadherin-OE + IRS-1 group, the relative protein expression of p-SHP2 was significantly decreased in the EGF + E-Cadherin-OE + benzyl butyl phthalate group, the relative protein expression of ZEB1 and α3-integrin was significantly increased, and the relative protein expression of E-Cadherin, p-Src, p-SMAD2, Snail and Slug showed no significant changes in their relative protein expression levels (Fig. 3). Therefore, it can be inferred from the above results that E-Cadherin inhibits the activation of Src by the EGF/SHP2/ZEB1/α3-integrin signaling pathway, thus preventing the EMT process in ovarian cancer cells.

E-Cadherin overexpression inhibits the EGF/SHP2/ZEB1/α3-integrin signaling pathway thereby inhibiting the migration and invasion of ovarian cancer cells

Therefore, we continued to explore the position and workings of E-Cadherin in sick ovarian cells. The cell scratch test revealed that in relation to the control group the wound closure rate was significantly higher in the EGF group. Concerning the wound closure rate, the EGF group had a higher rate than the EGF + E-Cadherin-OE group, which indicated a lower cell healing rate in the latter. Compared with the EGF + E-Cadherin-OE group, the wound closure rate of EGF + E-Cadherin-OE + IRS-1 and the EGF + E-Cadherin-OE + benzyl butyl phthalate group were significant increased. Moreover, the status of wound closure rate remains unchanged in the EGF + E-Cadherin-OE + IRS-1 group as well as EGF + E-Cadherin-OE + benzyl butyl phthalate group.

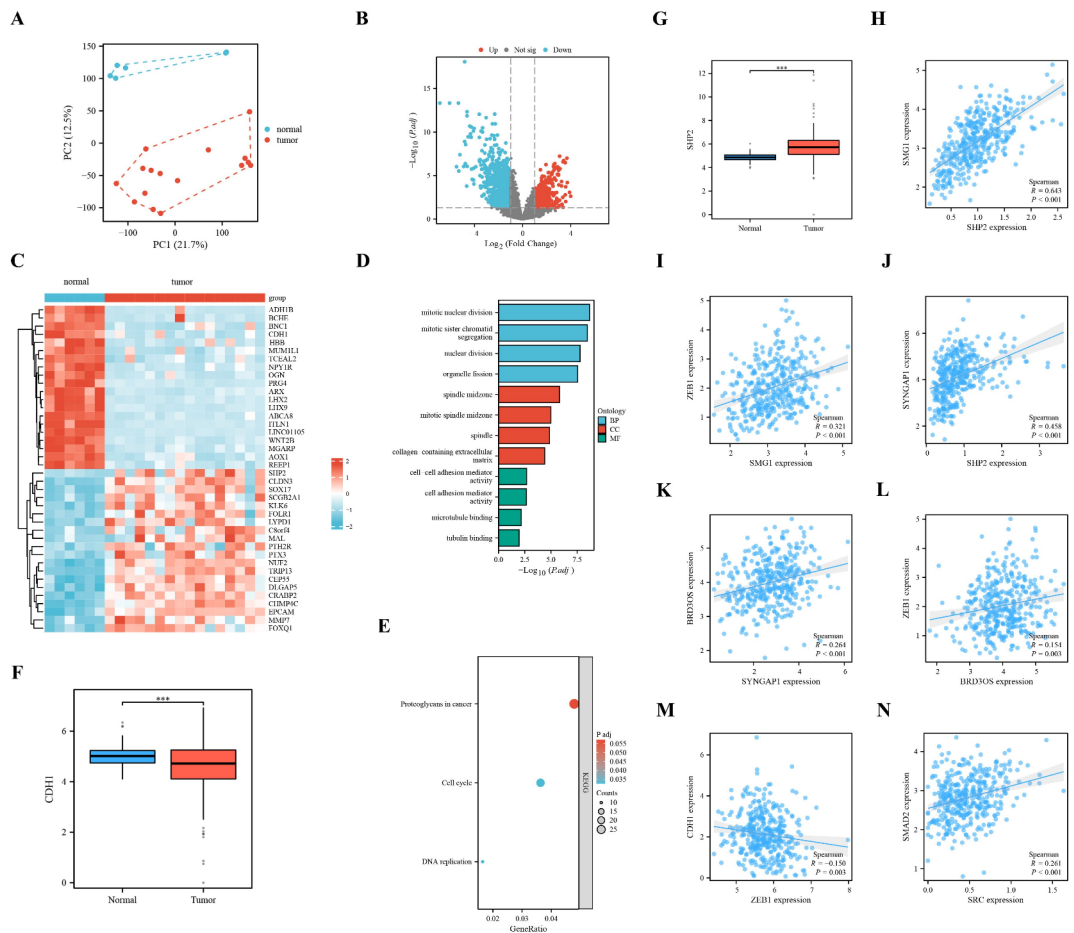


Fig. 1. Bioinformatics analysis. (A) Dataset calibration PCA plot; (B) Volcano plot of differentially expressed genes; (C) Heatmap of differentially expressed genes; (D) GO enrichment analysis histogram; (E) KEGG enrichment analysis bubble plot; (F) Expression analysis of E-Cadherin (CDH1) in normal tissues and OC tissues based on the GEO database; (G) Expression analysis of SHP2 in normal tissues and OC tissues based on the GEO database; (H) SHP2 and PI3K correlation scatter plot; (I) PI3K and ZEB1 correlation scatter plot; (J) SHP2 and RAS correlation scatter plot; (K) RAS and ERK1/2 correlation scatter plot; (L) ERK1/2 and ZEB1 correlation scatter plot; (M) ZEB1 and E-Cadherin correlation scatter plot; (N) Src and SMAD2 correlation scatter plot.

According to Transwell experiment results, differences between the densities of migrated and invaded cells rate in the EGF group and the control group were significantly increased. The data shown in Fig. 4 clearly indicate that several days after culture the density of migrated and invaded cells rate in the EGF + E-Cadherin-OE group was much lower than that in the EGF group. Compared to EGF + E-Cadherin-OE group, numbers of migrated and invaded cells rate as observed in EGF + E-Cadherin-OE + IRS-1 group and EGF + E-Cadherin-OE + benzyl butyl phthalate group were significantly higher. The migrated and invaded cells rate of the EGF + E-Cadherin-OE + IRS-1 group and EGF + E-Cadherin-OE + benzyl butyl phthalate group were insignificantly different as well (Fig. 4). Thus, the present study provides evidence that E-Cadherin can suppress the epithelial-mesenchymal transition by suppressing phosphorylation of ZEB1/α3-integrin nodes at every stage of the EGF/SHP2/ZEB1/α3-integrin signaling pathway and therefore the migration and invasion of ovarian cancer cells.

E-Cadherin overexpression promotes the progression of ovarian cancer and inhibits the expression of p-SHP2 and ZEB1 in tumors

Finally, we first injected SKOV3 cells by using the methods above and then we constructed E-Cadherin overexpression SKOV3 cells, and established the nude mice model of ovarian cancer by the subcutaneous injection of tumor cells into BALB/c nude mice. The results showed a significant reduction in tumor volume in the EGF + E-Cadherin-OE group compared to the EGF group. Next, the HE staining led to the finding of reduced tumor section area in the EGF + E-Cadherin-OE group compared to the EGF group. Immunohistochemical staining also exhibited that in the EGF + E-Cadherin-OE group, the p-SHP2-positive cells rate and ZEB1-positive cells rate was obviously down-regulated; in contrast, that of E-Cadherin-positive cells rate was evidently up-regulated compared with the EGF group (Fig. 5). The above results suggest that tyrosine phosphatase SHP2

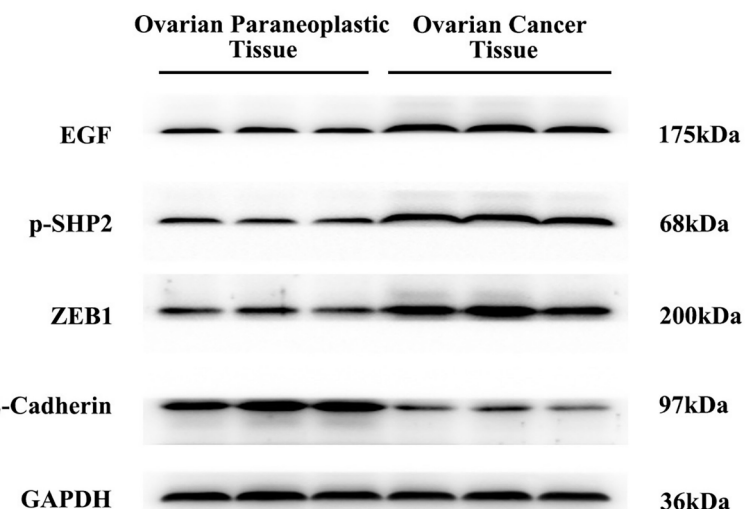
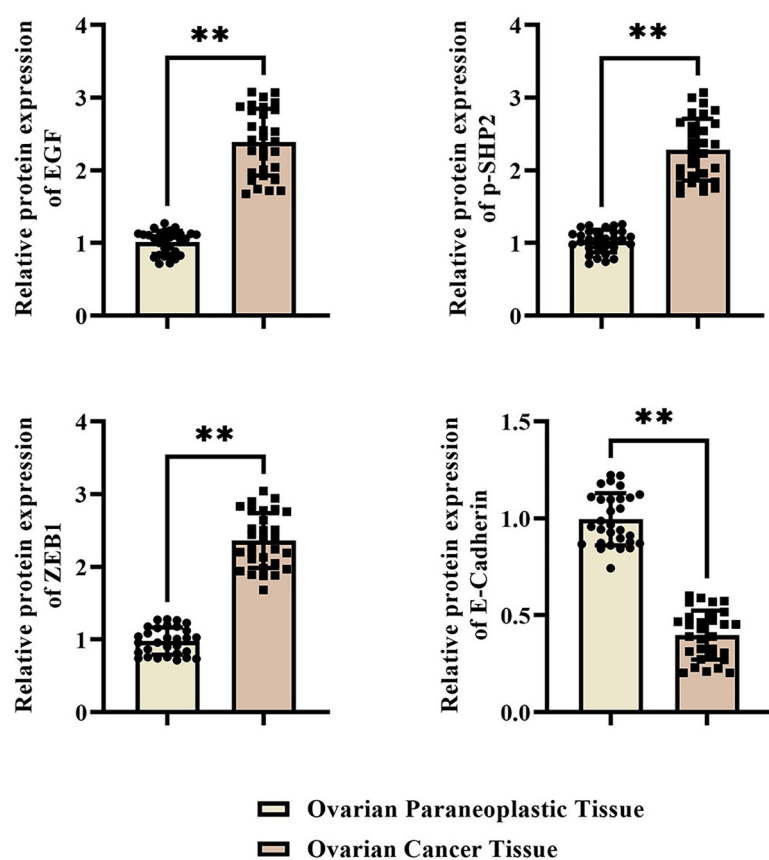
A**B**

Fig. 2. The EGF/SHP2/ZEB1 signaling pathway is activated and E-Cadherin is abnormally low in human ovarian cancer tissues. (A) Western blot analysis of the protein bands of EGF, p-SHP2, ZEB1 and E-Cadherin; (B) Statistical analysis of the relative protein expression levels of EGF, p-SHP2, ZEB1 and E-Cadherin. GAPDH was used as a control protein. Data are expressed as mean \pm standard deviation. $N=30$, $P<0.05$ is considered statistically significant. $^{**}P<0.01$.

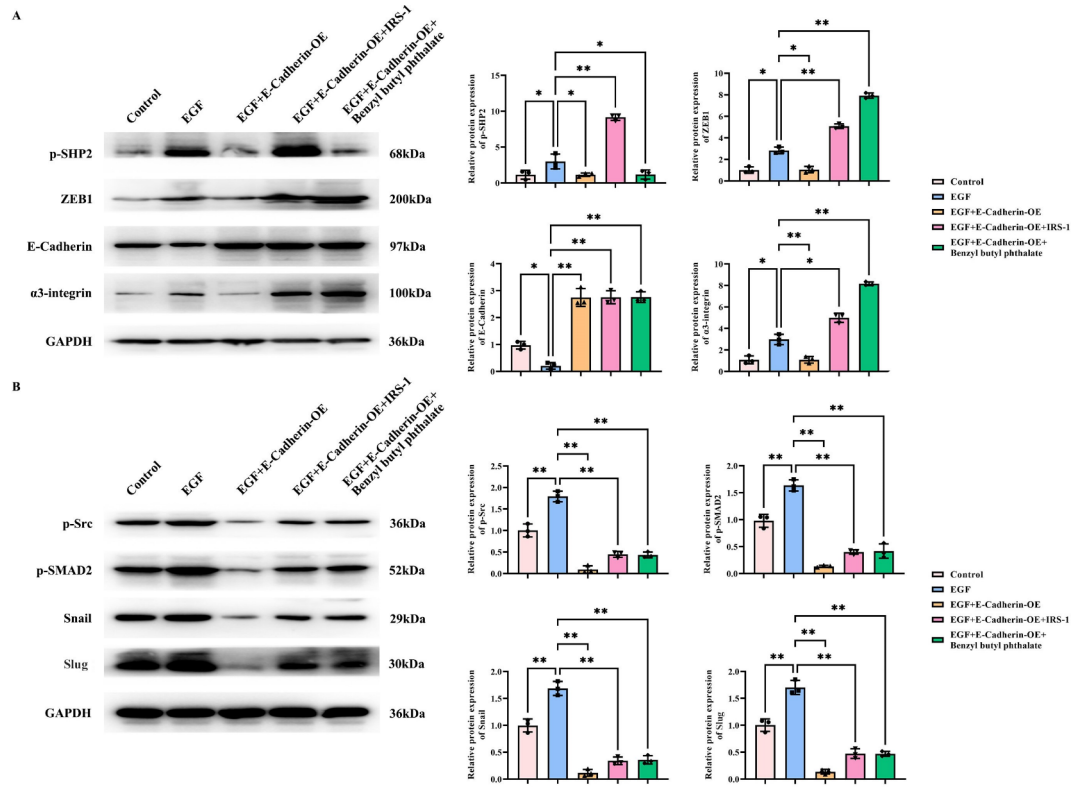


Fig. 3. E-Cadherin overexpression inhibits the EGF/SHP2/ZEB1/ α 3-integrin signaling pathway in ovarian cancer cells thereby inhibiting the EMT process. (A) Western blot analysis of the protein bands and relative protein expression levels of p-SHP2, ZEB1, E-Cadherin and α 3-integrin; (B) Western blot analysis of the protein bands and relative protein expression levels of p-Src, p-SMAD2, Snail and Slug. GAPDH is used as a control protein. Data are expressed as mean \pm standard deviation. $N=3$, $P < 0.05$ is considered statistically significant. $*P < 0.05$; $**P < 0.01$.

accelerates EMT by regulating the integrin/E-Cadherin balance mediated by the ZEB1 signal, thereby promoting the progression of ovarian cancer (Fig. 6).

Discussion

In the female reproductive system, ovarian cancer stands as the most malignant and lethal tumor. The ovaries are situated deep within the pelvic cavity, enveloped by the greater omentum and surrounded by the intestines. Consequently, early symptoms of ovarian disease are challenging to discern. Most patients receive their initial diagnosis of advanced ovarian cancer, often accompanied by infiltration of neighboring organs or distant metastasis, which significantly hinders the efficacy of treatment and diminishes the likelihood of recovery. Hence, there is an urgent demand for the identification of novel and effective molecular markers to facilitate the diagnosis and outcome prediction of ovarian cancer^{2,13}.

The primary mechanisms through which ovarian cancer metastasizes are direct invasion and implantation on the peritoneum. To date, a comprehensive understanding of the process by which cancer spreads to other body parts remains elusive. Recent studies have increasingly reported that epithelial-mesenchymal transition (EMT) is closely associated with the invasion and metastasis of epithelial ovarian cancer. EMT is a biological process wherein epithelial cells acquire mesenchymal characteristics under specified physiological or pathological conditions, leading to a loss of intercellular adhesion and an increase in migratory capacity. Notably, the reduction in E-Cadherin expression serves as a prominent indicator of EMT. E-Cadherin, a member of the cadherin family, plays a crucial role in maintaining the polarity and structural integrity of epithelial cells. During the malignant transformation and progression of various cancers, the down-regulation of E-Cadherin results in a loss of intercellular adhesion, both at the mRNA and protein levels^{14–16}.

Epidermal growth factor (EGF) is a focus in the study of tumor genesis and progression. EGF is a polypeptide comprising 53 amino acid residues, encoded by the gene located at human chromosome 4q25-27, and is present in diverse human tissues, as well as in the blood, urine, saliva, and tumor tissues of many cancer patients. This compound exhibits a wide range of biological activities: it can elevate intracellular metabolic rates, modify the cytoskeleton, stimulate protein synthesis, induce proto-oncogene activation, and promote cell differentiation and proliferation. Upon activation, the EGF receptor (EGFR) undergoes autophosphorylation on tyrosine residues, creating a docking site for the phosphotyrosine-binding domain of adaptor proteins. In EGF-stimulated cells, protein tyrosine phosphatase SHP2 is the principal binding partner of Grb2-related binder-1 (Gab1), with the

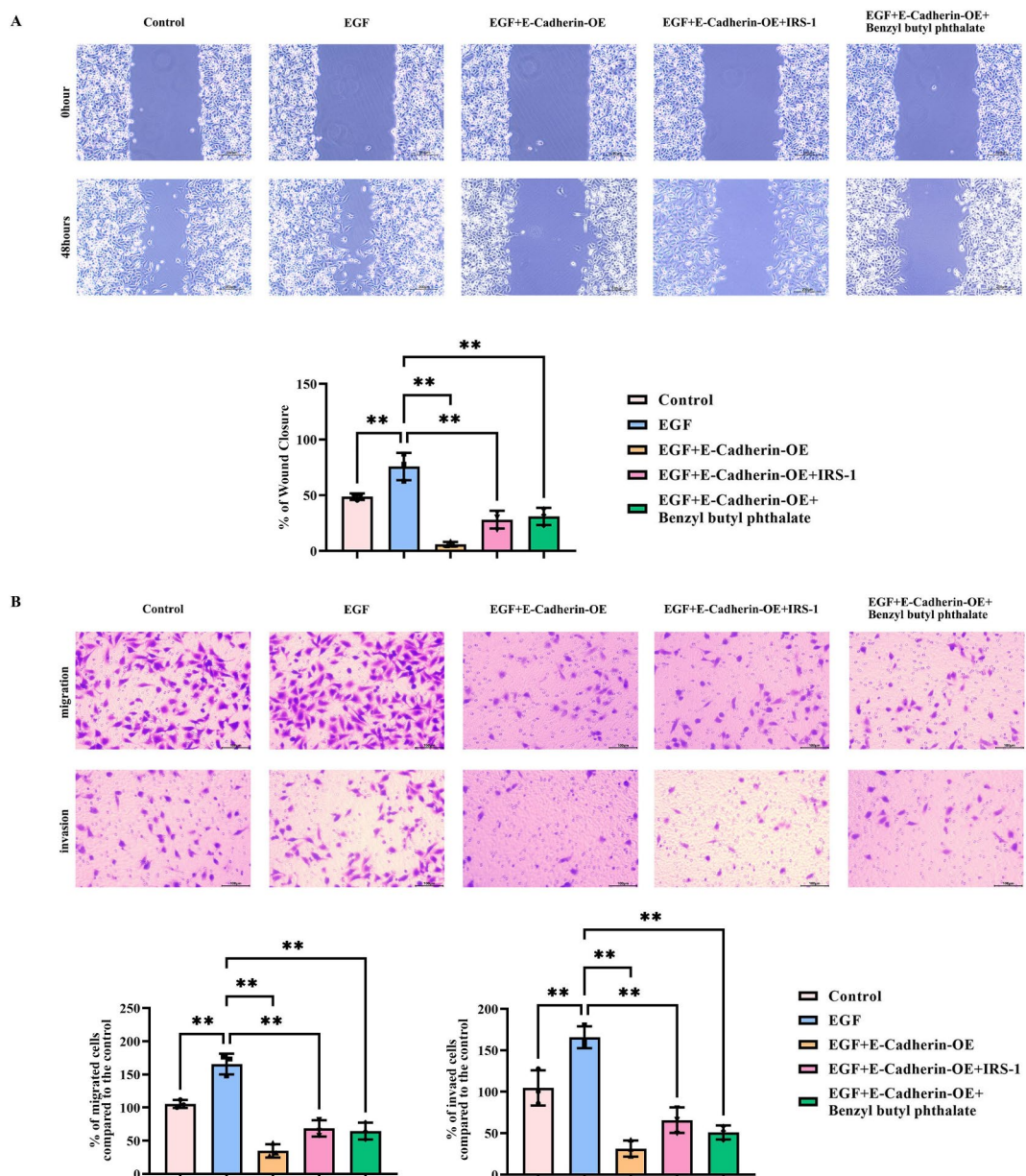


Fig. 4. E-Cadherin overexpression inhibits the EGF/SHP2/ZEB1/α3-integrin signaling pathway thereby inhibiting the migration and invasion of ovarian cancer cells. **(A)** Cell scratch assay was used to detect the migratory ability of SKOV3 cells; **(B)** Transwell assay was used to detect the migration and invasion ability of SKOV3 cells. Data are expressed as mean \pm standard deviation. $N=3$, $P<0.05$ is considered statistically significant. $*P<0.05$; $**P<0.01$.

tyrosine phosphorylation sites Tyr(P)-627 and Tyr(P)-659 of Gab1 forming a dual phosphorylated tyrosine-based activation motif (BTAM) that binds and activates SHP2. SHP2, encoded by the human PTPN11 gene, is a ubiquitously expressed non-receptor protein tyrosine phosphatase featuring two N-terminal Src homology 2 (SH2) domains, a protein tyrosine phosphatase catalytic domain, and a C-terminal tail. Mutants of SHP2 exhibit enhanced binding affinity to some of its target proteins, such as growth factor receptor-bound protein 1 (GAB1), contributing to the persistent Ras-mediated activation of ERK in response to growth factors. ERK1/2, a member of the MAPK family, is involved in numerous cellular pathways, including cell growth, development, and survival^{10,17,18}.

ZEB1 (zinc finger enhancer-binding protein 1) is a transcription factor that drives EMT, a process in which cells transform into mesenchymal cells, essential for development, tissue repair, and cancer metastasis. ZEB1 exerts a significant influence on EMT by enhancing the motility and invasiveness of cancer cells through the modulation of downstream target genes. Gab2, a well-known signal transduction adaptor protein, participates in multiple cellular signaling pathways. Gab2 can bind to phosphatidylinositol 3-kinase (PI3K) via a specific domain, thereby activating the PI3K/Akt signaling pathway, though it does not engage the MAPK pathway. Upon

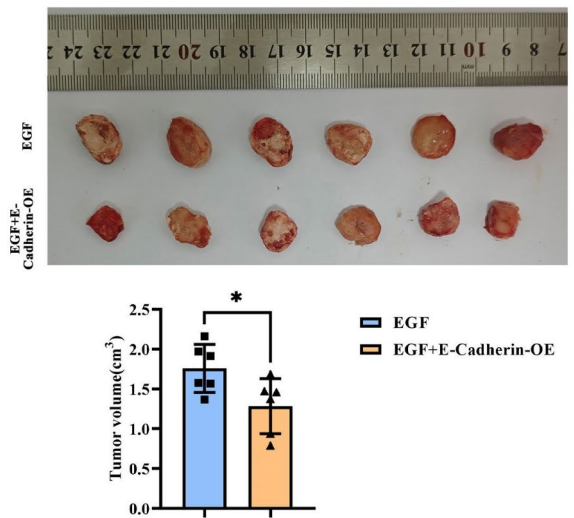
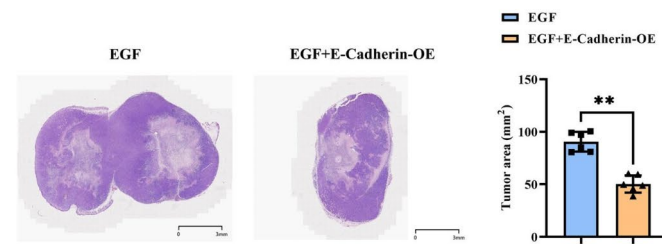
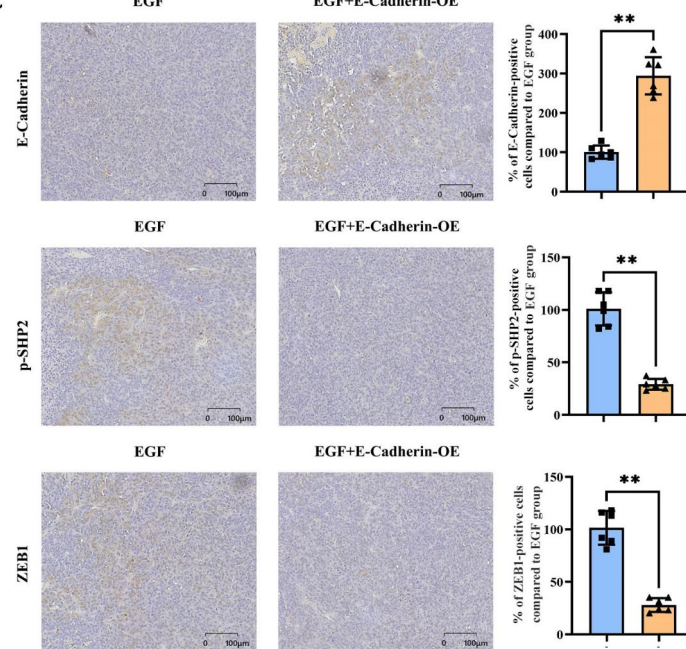
A**B****C**

Fig. 5. E-Cadherin overexpression promotes the progression of ovarian cancer and inhibits the expression of p-SHP2 and ZEB1 in tumors. (A) Statistical graph of tumor volume detected by subcutaneous graft tumor experiments in nude mice; (B) HE staining was used to detect the tumor tissue section area; (C) Immunohistochemical staining was used to detect the expression of p-SHP2, ZEB1 and E-Cadherin in tumor tissues. Data are expressed as mean \pm standard deviation. $N=6$, $P<0.05$ is considered statistically significant. $^{**}P<0.01$.

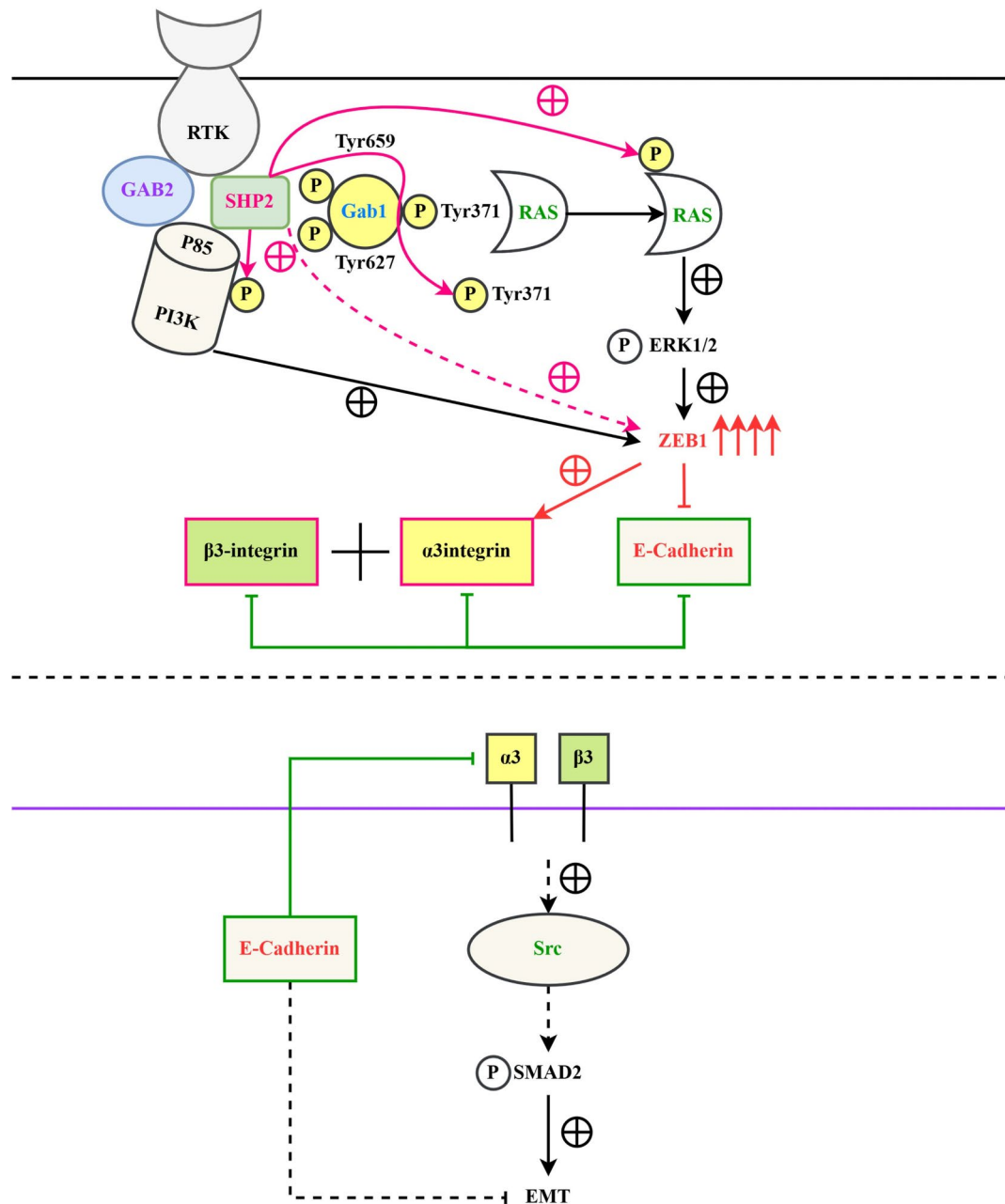


Fig. 6. Tyrosine phosphatase SHP2 accelerates EMT through regulating the integrin/E-Cadherin balance mediated by the ZEB1 signal, thereby promoting the progression of ovarian cancer.

activation, PI3K adds a phosphate group to phosphatidylinositol-4,5-bisphosphate (PIP2) at the 3-position, converting it into phosphatidylinositol-3,4,5-trisphosphate (PIP3). PIP3 subsequently recruits and activates Akt, also known as protein kinase B. Activated Akt regulates a plethora of cellular processes, such as proliferation, survival, and metabolism, by directly phosphorylating or indirectly activating other signaling molecules. During the EMT process, Akt can augment the levels of ZEB1 mRNA and protein or enhance its function. The activation of transcription factors like AP-1 and ETS family members by the ERK1/2 signaling pathway enables these factors to bind to the promoter region of the ZEB1 gene, thereby increasing its transcriptional activity. ZEB1 can physically interact with sequences in the promoter region of the E-Cadherin gene (CDH1), specifically its zinc finger domain, which binds to the E-box sequence on the E-Cadherin promoter, thereby displacing transcriptional activators and suppressing E-Cadherin transcription^{19–21}. In this study, the expression levels of EGF, p-SHP2, and ZEB1 were significantly higher in human ovarian cancer tissues compared to normal tissues, while E-Cadherin expression was notably lower.

On one hand, ZEB1, an important transcription factor, can suppress the expression of epithelial markers such as E-Cadherin. On the other hand, it has been observed that ZEB1 can also upregulate the expression of certain molecules involved in cell migration and invasion, including α 3-integrin and β 3-integrin. Integrins,

transmembrane receptors that mediate signaling between cells and the extracellular matrix (ECM), regulate cell adhesion, migration, and signal transduction²².

ZEB1 may interact directly or indirectly with the gene regulatory elements, such as promoter regions, of integrin subunits, thereby activating the transcription of these genes. Through this transcriptional activation, ZEB1 enhances the mRNA levels of α 3-integrin and β 3-integrin, ultimately increasing the protein expression of these integrins on the cell membrane. Following the binding of α 3-integrin and β 3-integrin to the extracellular matrix (ECM), they recruit and activate Src kinase. The activation of Src kinase initiates multiple downstream signaling pathways, which are involved in the regulation of cell adhesion, invasion, and epithelial-mesenchymal transition (EMT). Among these pathways, the TGF- β /SMAD pathway plays a particularly crucial role. The TGF- β signaling pathway is a key regulatory pathway for EMT. Upon the interaction of TGF- β with its receptor, the receptor is activated and phosphorylated, subsequently activating downstream SMAD proteins. The activation of Src kinase can enhance the activity of the TGF- β receptor, thereby facilitating the activation and phosphorylation of SMAD2. The activated SMAD2 translocates to the nucleus and interacts with other SMAD proteins and transcription factors to either induce the expression or modulate the activity of EMT transcription factors, such as ZEB1, Snail, and Slug. These transcription factors concurrently reduce the levels of epithelial markers, such as E-Cadherin, while increasing the levels of mesenchymal markers, like N-cadherin and Vimentin, further promoting the EMT process²³⁻²⁵. As a cell adhesion molecule, E-Cadherin typically decreases in expression during EMT, thereby stimulating cell migration and invasiveness and improving prognosis. Bioinformatics analysis identified 21,655 significantly differentially expressed genes (DEGs) using DESeq2, of which 643 were upregulated and 840 were downregulated. Furthermore, it was revealed that CDH1 was downregulated while SHP2 was upregulated in ovarian cancer (OC) tissues. Gene Ontology (GO) and Kyoto Encyclopedia of Genes and Genomes (KEGG) pathway analysis demonstrated that these DEGs were primarily involved in the cell cycle, DNA replication, and cancer-related pathways. Data from the Gene Expression Omnibus (GEO) database corroborated the findings of SHP2 upregulation and CDH1 downregulation in OC samples. Correlation analysis indicated that SHP2 promotes the expression of PI3K (SMG1), which in turn influences the expression of ZEB1. Concurrently, SHP2 also enhances the expression of RAS (SYNGAP1) and ERK1/2 (BRD3OS). The interactions among these factors result in the repression of E-Cadherin (CDH1) by ZEB1, and Src promotes the expression of SMAD2. Experimental studies have demonstrated that E-Cadherin not only directly affects cell adhesion but also indirectly regulates various molecules associated with cell migration and invasion, including α 3-integrin and β 3-integrin. The ligation of E-Cadherin to β -catenin on the cell membrane prevents β -catenin from translocating to the nucleus and activating the Wnt signaling pathway. Therefore, the Wnt signaling pathway plays a regulatory role in EMT and integrin expression. The presence of E-Cadherin inhibits Wnt signal transduction, thereby indirectly reducing the expression of α 3-integrin and β 3-integrin. E-Cadherin can also decrease the dependence on integrin-based cell adhesion to the ECM, thus suppressing the action and synthesis of α 3-integrin and β 3-integrin. It has been found that the expression of E-Cadherin in epithelial cells is inversely correlated with the expression of integrin subunits. This study shows that under conditions of E-Cadherin deficiency or reduced expression, cells exhibit higher expression levels of α 3-integrin and β 3-integrin, suggesting that overexpression of E-Cadherin may suppress the expression of these integrins through the aforementioned mechanisms. Western blot analysis revealed that the expression of p-SHP2, ZEB1, α 3-integrin, p-Src, p-SMAD2, Snail, and Slug proteins in ovarian cancer cells stimulated by EGF was downregulated, while the expression of E-Cadherin was upregulated. This enhancement can boost the migration and invasion capability of SKOV3 cells. Once the aforementioned protein targets are specifically upregulated by E-Cadherin, the protein expression levels of p-SHP2, ZEB1, α 3-integrin, p-Src, p-SMAD2, Snail, and Slug increase, and the migration and invasiveness of SKOV3 cells are simultaneously alleviated. Treatment with IRS-1 and benzyl butyl phthalate counteracts the suppression of E-Cadherin on the EMT process induced by α 3-integrin and β 3-integrin signaling, leading to a significant enhancement in the migration and invasion capability of SKOV3 cells. In vivo experiments confirmed that E-Cadherin overexpression can inhibit ovarian cancer metastasis, and the expression levels of p-SHP2 and ZEB1 in tumor tissues are substantially suppressed.

In summary, our study confirmed that SHP2 is a prognostic indicator for ovarian cancer patients, and the experimental results suggest that the tyrosine phosphatase SHP2 accelerates EMT by regulating the integrin/E-Cadherin balance mediated by the ZEB1 signal, thus implementing the advancement of ovarian cancer. It offers potential biomarkers and ideas for the research focused on the treatment of ovarian carcinoma. However, there are some limitations of our study. The sample size of our study was relatively small, and future studies should increase the sample size to improve the reliability of the results. Although we demonstrated the mechanism by which SHP2 regulates EMT through the integrin/E-Cadherin/ZEB1 pathway, its specific molecular details and downstream targets remain to be further explored.

Data availability

The datasets generated during and/or analysed during the current study are available from the corresponding author on reasonable request.

Received: 8 August 2024; Accepted: 2 January 2025

Published online: 09 January 2025

References

1. Xiao, Y. et al. Multi-omics approaches for biomarker discovery in early ovarian cancer diagnosis. *EBioMedicine* **79**, 104001 (2022).
2. Yang, C. et al. Immunotherapy for ovarian cancer: adjuvant, combination, and neoadjuvant. *Front. Immunol.* **11**, 577869 (2020).
3. Wang, L. et al. Drug resistance in ovarian cancer: from mechanism to clinical trial. *Mol. Cancer* **23** (1), 66 (2024).

4. Liu Y N, Guan, Y. et al. Shp2 positively regulates cigarette smoke-induced epithelial mesenchymal transition by mediating MMP-9 production. *Respir. Res.* **21** (1), 161 (2020).
5. Wang L N, Zhang Z T, Wang, L. et al. TGF- β 1/SH2B3 axis regulates anoikis resistance and EMT of lung cancer cells by modulating JAK2/STAT3 and SHP2/Grb2 signaling pathways. *Cell Death Dis.* 13472 (2022).
6. Li, T. et al. Gab1 regulates invadopodia and autocrine VEGF through SHP2/ERK1/2 in hilar cholangiocarcinoma cells. *Am. J. Transl. Res.* **14** (12), 8934–8946 (2022).
7. Wei, L. et al. miRNA-199b-3p suppresses growth and progression of ovarian cancer via the CHK1/E-cadherin/EMT signaling pathway by targeting ZEB1. *Oncol. Rep.* **45** (2), 569–581 (2021).
8. Wang, X. et al. SNX10-mediated LPS sensing causes intestinal barrier dysfunction via a caspase-5-dependent signaling cascade. *EMBO J.* **40** (24), e108080 (2021).
9. Aban, C. E. et al. Downregulation of E-cadherin in pluripotent stem cells triggers partial EMT. *Sci. Rep.* **11** (1), 2048. (2021).
10. Wang, Q. et al. Protein tyrosine phosphatase SHP2 suppresses host innate immunity against influenza A Virus by regulating EGFR-mediated signaling. *J. Virol.* **95** (6), (2021).
11. Hartman, Z., Geldenhuys W J, Agazie & Y M. A specific amino acid context in EGFR and HER2 phosphorylation sites enables selective binding to the active site of src homology phosphatase 2 (SHP2). *J. Biol. Chem.* **295** (11), 3563–3575 (2020).
12. Zhang, L. et al. SHP-2-mediated upregulation of ZEB1 is important for PDGF-B-induced cell proliferation and metastatic phenotype in triple negative breast cancer. *Front. Oncol.* **10**, 1230 (2020).
13. Zhang, R. et al. Molecular biomarkers for the early detection of ovarian cancer. *Int. J. Mol. Sci.* **23**(19). (2022).
14. Xu, S. et al. ARID1A restrains EMT and stemness of ovarian cancer cells through the hippo pathway. *Int. J. Oncol.* **65**(2). (2024).
15. Chen, Q. et al. MAP7 drives EMT and cisplatin resistance in ovarian cancer via wnt/ β -catenin signaling. *Helix* **10** (9), e30409 (2024).
16. Xie, W. et al. OCT4 induces EMT and promotes ovarian cancer progression by regulating the PI3K/AKT/mTOR pathway. *Front. Oncol.* **12**, 876257 (2022).
17. Tang K H, Li, S. et al. Combined inhibition of SHP2 and CXCR1/2 promotes antitumor T-cell response in NSCLC. *Cancer Discov.* **12** (1), 47–61 (2022).
18. Kanumuri, R. et al. Targeting SHP2 phosphatase in hematological malignancies. *Expert Opin. Ther. Targets* **26** (4), 319–332 (2022).
19. SÁNCHEZ-TILLÓ, E. et al. The EMT factor ZEB1 paradoxically inhibits EMT in BRAF-mutant carcinomas. *JCI Insight* **8**(20). (2023).
20. Cheng, Z. & Sun, W. GAB2 inhibits chondrocyte apoptosis through PI3K-AKT signaling in osteoarthritis. *Int. J. Clin. Exp. Pathol.* **13** (3), 616–623 (2020).
21. Tian, J. & Zhang, H. The miR-218/GAB2 axis regulates proliferation, invasion and EMT via the PI3K/AKT/GSK-3 β pathway in prostate cancer. *Exp. Cell Res.* **394** (1), 112128 (2020).
22. Wu H T et al. Oncogenic functions of the EMT-related transcription factor ZEB1 in breast cancer. *J. Transl. Med.* **18** (1), 51 (2020).
23. Zhao, X. et al. Polydatin inhibits ZEB1-invoked epithelial-mesenchymal transition in fructose-induced liver fibrosis. *J. Cell. Mol. Med.* **24** (22), 13208–13222 (2020).
24. Li, K. et al. Desmosomal proteins of DSC2 and PKP1 promote cancer cells survival and metastasis by increasing cluster formation in circulatory system. *Sci. Adv.* **7** (40), eabg7265 (2021).
25. Liu, H. et al. MiR-194-5p inhibited metastasis and EMT of nephroblastoma cells through targeting crk. *Kaohsiung J. Med. Sci.* **36** (4), 265–273 (2020).

Author contributions

X.F.L conceived and designed the experiment. H.B.Z and J.N.D performed cell cultures and completed the experiments. J.W for data analysis. All authors read and approved the final manuscript.

Funding

This study was funded by a project of the Hebei Provincial Department of Health. (Project number:20221262).

Declarations

Competing interests

The authors declare no competing interests.

Ethics approval

This study was reviewed and approved by the Ethics Committee for Laboratory Animal Welfare of the Fourth Hospital of Hebei Medical University. Date: 2024.01.20. (No.20240721).

Additional information

Supplementary Information The online version contains supplementary material available at <https://doi.org/10.1038/s41598-025-85445-w>.

Correspondence and requests for materials should be addressed to J.W.

Reprints and permissions information is available at www.nature.com/reprints.

Publisher's note Springer Nature remains neutral with regard to jurisdictional claims in published maps and institutional affiliations.

Open Access This article is licensed under a Creative Commons Attribution-NonCommercial-NoDerivatives 4.0 International License, which permits any non-commercial use, sharing, distribution and reproduction in any medium or format, as long as you give appropriate credit to the original author(s) and the source, provide a link to the Creative Commons licence, and indicate if you modified the licensed material. You do not have permission under this licence to share adapted material derived from this article or parts of it. The images or other third party material in this article are included in the article's Creative Commons licence, unless indicated otherwise in a credit line to the material. If material is not included in the article's Creative Commons licence and your intended use is not permitted by statutory regulation or exceeds the permitted use, you will need to obtain permission directly from the copyright holder. To view a copy of this licence, visit <http://creativecommons.org/licenses/by-nc-nd/4.0/>.

© The Author(s) 2025